# UNCERTAINTY ON SIGNAL PARAMETER ESTIMATION IN FREQUENCY DOMAIN

*Consolatina Liguori*

Department of Automation, Electromagnetism, Information Engineering and Industrial Mathematics, DAEIMI, University of Cassino, Italy

**Abstract** – *In the paper the analytical evaluation of the uncertainty on signal parameter estimation in frequency domain is dealt with. Two different and widely diffused algorithms able to compensate the spectral leakage effects due to asynchronous sampling are considered. The combined uncertainties on the final results (tones frequency, amplitude, and phase) due to the propagation of the uncertainty on the input samples are analytically evaluated. Simulation tests are then carried out in order to validate the obtained formulas.*

**Keywords -** Uncertainty analysis, FFT, Interpolated FFT, algorithm uncertainty, spectral leakage.

## 1. INTRODUCTION

A measurement result to be usable (comparable with other measurement results or with reference value) needs a quantitative indication of its reliability and quality. In fact, since no measurement is perfect, its result is only an approximation to the value of the measurand and consequently the quality of the approximation has to be indicated [1].

In particular, the *Guide to the expression of Uncertainty in Measurement* (*GUM*) [1] standardises the measurement quality expression, defining the uncertainty as "a parameter, associated with the result of a measurement, that characterises the dispersion of the values that could reasonably be attributed to the measurand". The uncertainty completely describes the measurement reliability if the result is corrected for all known systematic effects *(bias)* that significantly influence the estimation.

Bias and uncertainty of a measurement value are not always easy to be estimated, especially when they concern measurement obtained by digital elaboration of sampled signals. In fact, the metrological characteristics of digital-signal-processing-based instruments depend not only on the hardware configuration but also and mainly on the specific software [2].

In the field of the spectral waveform analysis, digital techniques are very diffuse, especially for real-time application and/or for signal parameter estimation. The continuos Fourier transform is approximate by means of the discrete Fourier transform (DFT), implemented by the fast Fourier transform (FFT). To correctly use the resulting spectrum, as previously said, the user has to assess its accuracy.

Consequently, there is a great interest in the FFT results characterisation in terms of bias and uncertainty evaluation, as proved by the numerous and valuable paper found in literature. A world-wide discussion is open about deterministic errors that cause bias in the results [3]. Other fundamental studies concern the bias effects of the chosen window, of asynchronous sampling, of the finite duration of the sampling impulses on frequency, amplitude, and phase estimation [4]-[6]. Together with these error analyses, techniques or suitable elaboration are often suggested in order to eliminate or reduce the final bias of the results (*e.g.* interpolation techniques, advanced windows [7]-[10]).

The authors in [11] already tackled the problem of the analytical evaluation of DFT and FFT output data uncertainty, according to the GUM. They used a method based on a "white box" theoretical approach [2]. With reference to main sources of uncertainty (quantization, time jitter, microprocessor finite wordlength), they identified equations useful to evaluate the uncertainty in both module and phase output values, for any hardware configuration and for any algorithm operating condition (e.g. window used, number of points).

In the case of synchronous sampling, the amplitude and phase tones uncertainty is equal to the uncertainty of the corresponding estimated DFT sample. Vice versa, in the case of asynchronous sampling, the spectral leakage, causes deterministic error on the tones frequency amplitude and phase evaluation, consequently the above equalities are not valid. To extend the results obtain in [11] also for the signal parameter estimation in case of asynchronous sampling, it is indispensable to take into account the effect of spectral leakage and harmonic interference.

Some methods are reported in literature that allow deterministic errors on frequency, amplitude and phase due to the spectral leakage to be corrected [7], [8], [10]. They allow the deterministic error to be practically zeroed, whereas uncertainty still affects the measurement results due to both the uncertainty on the FFT samples and the one on the correction algorithm.

In this paper, two different algorithms for signal parameter estimation in frequency domain [7], [8], [10] will be characterised with reference to the obtainable uncertainty.

For both algorithms, the uncertainty on the final results (tones frequency, amplitude and phase) will be evaluated combining the uncertainty of each FFT sample as in [11] and the uncertainty introduced by the specific correction algorithm. The obtained analytical formulas will be then numerically verified by simulation. Furthermore comparison between the two approaches will be presented with reference to different operating conditions.

ISBN 972-98115-4-7  

## 2. THE MEASUREMENT ALGORITHMS

The DFT of an N-point sequence {x(n)} weighted with a window function {w(n)} is defined as:

$$X(k) = \frac{1}{S}\sum_{n=0}^{N-1} w(n)\cdot x(n)\ e^{-jk\beta_n} \quad k = 0...N-1, \tag{1}$$

where $S = \sum_{n=0}^{N-1} w(n)$ and $\beta_n = \frac{2\pi n}{N}$. Posing:

$$R(k) = \frac{1}{S}\sum_{n=0}^{N-1} w(n)x(n)\cos(k\beta_n);\ I(k) = \frac{1}{S}\sum_{n=0}^{N-1} w(n)x(n)\sin(k\beta_n) \tag{2}$$

the following states: $X(k) = R(k) - jI(k)$ and, consequently, the module M(k) and the phase φ(k) of each frequency domain sample X(k) are given respectively by:

$$M(k) = \sqrt{R^2(k)+I^2(k)}; \tag{3}$$

$$\varphi(k) = -arctg\left(\frac{I(k)}{R(k)}\right). \tag{4}$$

In case of synchronous sampling, namely if for a multi-frequency signal $x(t) = \sum_i A_i \sin(2\pi f_i t + \gamma_i)$ all the signal components, $f_i$, are multiple of the frequency resolution, Δf: $f_i = k_i\,\Delta f$ (with $k_i \in N$), the amplitude and phase of the $i^{th}$ tones can be directly derived from the $k_i^{th}$ sample of the signal DFT, M(k), φ(k).

Vice versa, in the case of asynchronous sampling (∃ i ∋' $f_i \neq k_i\,\Delta f$), the above stated relations are not valid because of the spectral leakage [9], that causes deterministic error on the tones frequency amplitude and phase evaluation.

The algorithms [7],[8],[10] for correcting the spectral leakage effects evaluate the frequency tones as:

$$f_i = (k_i + \delta_i)\Delta f \tag{5}$$

where $-1/2 \leq \delta_i < 1/2$, and $k_i$ correspond to the relative maxima in the amplitude spectrum.

Consequently, the implementation of these methods foresees a preliminary analysis of the amplitude spectrum to search these maxima. Then, for each maximum $k_i$, $\delta_i$ is evaluated and finally the tone frequency, amplitude and phase are calculated. Differences are present on the algorithm used to determine $\delta_i$ and to evaluate the tone amplitude and phase. In the following, two widely diffused algorithms are recalled.

The first one [7], [8] is based on an interpolation of the FFT output and consequently is often called Interpolated FFT (IFFT); it gives very good results once suitable windows are used. The second one [10] is based on the evaluation of certain energy parameters related to the spectral component, and is characterised by high accuracy even with a small number of samples.

Both methods are always applicable but a minimum frequency distance, Δλ, between two adjacent spectral components must be guaranteed. In fact tones very close to each other may cause spectral interference that can hide very low amplitude tones since the errors introduced in the tones parameter evaluation are heavier for the tone with lower amplitude.

### *2.1 Interpolated FFT*

For the spectral component $f_i$, the $\delta_i$ evaluation is carried out by considering the ratio, $\alpha_i$, between the two largest samples corresponding to the tone peak:

$$\alpha_i = \frac{M(k_i+\varepsilon_i)}{M(k_i)} \tag{5}$$

where

$$\varepsilon_i = \begin{cases} 1 & \text{if } M(k_i+1) \geq M(k_i) \\ -1 & \text{if } M(k_i+1) < M(k_i) \end{cases} \tag{6}.$$

Besides, considering the window frequency spectrum (W(k)), we have that [7], [8]:

$$\alpha_i = \frac{|W(\varepsilon_i - \delta_i)|}{|W(-\delta_i)|} \tag{7}.$$

By matching relationships (5) and (7), we can obtain $\delta_i$. The amplitude, $A_i$, and phase, $\gamma_i$, of the *i*th spectral component can be estimated as follows:

$$A_i = \frac{2M(k_i)}{|W(-\delta_i)|}; \tag{8}$$

$$\gamma_i = (k_i) - \arg(W(\delta_i)). \tag{9}$$

Even though the method does not impose any restriction on the window employed, direct relations can be obtained using the weighted cosine window [6], namely the window (w(n)) such that:

$$w(n) = \sum_{h=0}^{H-1} a_h \cos(h\beta_n). \tag{10}$$

where H is the number of the considered cosine terms.

In fact, for this class of window we have [7], [8]:

$$\alpha_i = \varepsilon_i \frac{(1-\varepsilon_i\cdot\delta_i)}{\delta_i}\cdot\frac{\left|\sum_{h=0}^{H-1}\frac{a_h}{(1-\varepsilon_i\cdot\delta_i)^2-h^2}\right|}{S_{\delta_i}}; \tag{11}$$

where:

$$S_{\delta_i} = \sum_{h=0}^{H-1}\frac{a_h}{\delta_i^2-h^2}. \tag{12}$$

$\delta_i$ are calculated inverting (11), whilst $A_i$ and $\gamma_i$ can be evaluated from (8) and (9) as:

$$A_i = \frac{2\cdot S}{N}\frac{\pi}{\delta_i\, sen(\pi\delta_i)}\frac{M(k_i)}{S_{\delta_i}} \tag{13}$$

$$\gamma_i = \varphi(k_i) + \frac{\pi}{2} - \pi\delta_i - m\pi\ ;\ m=0 \text{ if } S_{\delta i} > 0 \text{ else } m=1. \tag{14}$$

Table I reports the $a_i$ parameters and the relationship between $\alpha_i$ and $\delta_i$ for some windows [6].

### *2.2 Energy parameter-based algorithm*

It is based on the evaluation in the frequency domain of certain energy parameters related to each spectral component of the analysed signal [10].

At first the window energy parameter, $E_w$, is evaluated using the window DFT samples, W(k):

$$E_w = \sum_{k=0}^{N}|W(k)|^2. \tag{15}$$

Tab. I Characteristics of some windows

| **Window** | Rectangular | Hanning | 4-terms Nuttal |
|---|---|---|---|
| **H** | 1 | 2 | 4 |
| **Coefficients** | $a_0$=1 | $a_0$=1; $a_1$=-0.5 | $a_0$=10/32; $a_1$=-15/32; $a_0$=6/32; $a_1$=-1/32 |
| **$\delta_i$** | $\varepsilon_i\frac{\alpha_i}{1+\alpha_i}$ | $\varepsilon_i\frac{2\alpha_i-1}{1+\alpha_i}$ | $\varepsilon_i\frac{4\alpha_i-3}{1+\alpha_i}$ |

Then, for each $i^{th}$ detected tone on the signal spectrum, X(k), some quantities are evaluated, related to the $i^{th}$ spectral component energy, and in particular the energies of the tone, $E_{x_i}$, of the tone first derivative, $E_{xd_i}$, and of the conjugate symmetric of the tone $E_{xc_i}$:

$$E_{x_i} = \sum_{\ell \in B} M(k_i + \ell)^2 ; \quad (16)$$

$$E_{xd_i} = \sum_{\ell \in B} \ell \cdot M(k_i + \ell)^2 ; \quad (17)$$

$$E_{xc_i} = \sum_{\ell \in B} R(k_i + \ell)^2 \quad (18)$$

Since the window transform concentrates almost all its energy near its center frequency, these energy parameters can be evaluated on few spectral samples, taken in a very narrow frequency band, B, located around the peak. In particular, B≡[-K, K], where K is chosen as compromise between a good energy evaluation and a low Δλ.

The tone characteristics are obtained as:

$$\delta_0 = \frac{E_{xdi}}{E_{x_i}} ; \quad (19)$$

$$A_i = 2 \cdot S \sqrt{\frac{E_{x_i}}{E_w}} ; \quad (20)$$

$$\cos^2(\beta_i) = \frac{E_{ci}}{E_{xi}} . \quad (21)$$

## 3. THEORETICAL ESTIMATION OF UNCERTAINTY

To evaluated the combined standard uncertainty on the tone characteristics ($f_i$, $A_i$, $\gamma_i$), the uncertainty propagation law [1] is applied to the previously obtained equations, considering known the uncertainty on R(k), M(k), I(k) (see appendix A).

As far as the frequency uncertainty, $U_{f_i}$, is concern, if uncertainties on the sampling frequency and on the maximum positions $k_i$, are absent or negligible, from (5) we have:

$$U_{f_i}^2 = \Delta f^2 \cdot U_{\delta_i}^2 . \quad (22)$$

In the following for sake of brevity the phase uncertainty evaluation is not reported.

### *3.1 Interpolated FFT*

Frequency uncertainty. At first the uncertainty on each $\alpha_i$ is calculated from (6):

$$U_{\alpha_i}^2 = \left(\frac{\partial \alpha_i}{\partial M(k_i)}\right)^2 U_{M(k_i)}^2 + \left(\frac{\partial \alpha_i}{\partial M(k_i + \varepsilon_i)}\right)^2 U_{M(k_i+\varepsilon_i)}^2 + 2 \frac{\partial \alpha_i}{\partial M(k_i)} \cdot \frac{\partial \alpha_i}{\partial M(k_i + \varepsilon_i)} U\left(M(k_i), M(k_i + \varepsilon_i)\right) \quad (23)$$

where: $\frac{\partial \alpha_i}{\partial M(k_i)} = -\frac{M(k_i + \varepsilon_i)}{M^2(k_i)}$, $\frac{\partial \alpha_i}{\partial M(k_i + \varepsilon_i)} = \frac{1}{M(k_i)}$. (24)

(for $U\left(M(k_i), M(k_i + \varepsilon_i)\right)$ see B1).

The so obtained uncertainty is used to evaluate the uncertainty on $\delta_i$: $U_{\delta_i}^2 = \left(\frac{\partial \delta_i}{\partial \alpha_i}\right)^2 U_{\alpha_i}^2 = c_i^2 \cdot U_{\alpha_i}^2$. (25)

The sensitivity coefficient, $c_i$, strictly depends on the window used. Table II reports the values of $c_i$ for the same windows summarised in Tab. I.

Amplitude uncertainty. Applying the uncertainty propagation law to (13), and remembering that $\delta_i = f(\alpha_i) = g(M(k_i), M(k_i + \varepsilon_i))$ we have:

$$U_{A_i}^2 = \left(\frac{\partial A_i}{\partial M(k_i)}\right)^2 U_{M(k_i)}^2 + \left(\frac{\partial A_i}{\partial M(k_i + \varepsilon_i)}\right)^2 U_{M(k_i+\varepsilon_i)}^2 + 2 \frac{\partial A_i}{\partial M(k_i)} \cdot \frac{\partial A_i}{\partial M(k_i + \varepsilon_i)} U\left(M(k_i), M(k_i + \varepsilon_i)\right) \quad (26)$$

where from (13):

$$\frac{\partial A_i}{\partial M(k_i)} = \frac{2}{N} \cdot \frac{\pi}{\delta_i \operatorname{sen}(\pi \delta_i)} \cdot \frac{1}{S_{\delta_i}} + \frac{\partial A_i}{\partial \delta_i} \cdot \frac{\partial \delta_i}{\partial \alpha_i} \cdot \frac{\partial \alpha_i}{\partial M(k_i)} \quad (27)$$

$$\frac{\partial A_i}{\partial M(k_i + \varepsilon_i)} = \frac{\partial A_i}{\partial \delta_i} \cdot \frac{\partial \delta_i}{\partial \alpha_i} \cdot \frac{\partial \alpha_i}{\partial M(k_i + \varepsilon_i)} \quad (28)$$

$$\frac{\partial A_i}{\partial \delta_i} = -\frac{\operatorname{sen}(\pi \delta_i) + \pi \cos(\pi \delta_i)}{\delta_i^2 \operatorname{sen}^2(\pi \delta_i)} \cdot \frac{1}{S_{\delta_i}} + \frac{2}{N} \cdot \frac{\pi}{\delta_i \operatorname{sen}(\pi \delta_i)} \left[ \frac{2\delta_i}{S_{\delta_i}^2} \sum_{h=0}^{H-1} \frac{a_h}{(\delta_i^2 - h^2)^2} \right] \quad (29)$$

whereas for $\frac{\partial \alpha_i}{\partial M(k_i)}$ and $\frac{\partial \alpha_i}{\partial M(k_i + \varepsilon_i)}$ see (24).

### *3.2 Energy parameter-based algorithm*

Frequency uncertainty. From (19) we have:

$$U_{\delta_i}^2 = \sum_{\ell=-K}^{K} \left(\frac{\partial \delta_i}{\partial M(k_i + \ell)}\right)^2 U_{M(k_i+\ell)}^2 + 2 \sum_{\ell=-K}^{K-1} \sum_{r=\ell+1}^{K} \frac{\partial \delta_i}{\partial M(k_i + \ell)} \cdot \frac{\partial \delta_i}{\partial M(k_i + r)} U\left(M(k_i + \ell), M(k_i + r)\right) \quad (30)$$

where:

$$\frac{\partial \delta_i}{\partial M(k_i + \ell)} = \frac{1}{E_{x_i}^2} \left[ 2\ell M(k_i + \ell) E_{x_i} - 2 E_{xd_i} M(k_i + \ell) \right]. \quad (31)$$

Amplitude uncertainty. Considering the equation (20):

$$U_{A_i}^2 = \sum_{\ell=-K}^{K-1} \left(\frac{\partial A_i}{\partial M(k_i + \ell)}\right)^2 U_{M(k_i+\ell)}^2 + 2 \cdot \sum_{\ell=-K}^{K-1} \sum_{r=\ell+1}^{K} \frac{\partial A_i}{\partial M(k_i + \ell)} \frac{\partial \delta_i}{\partial M(k_i + r)} U\left(M(k_i + \ell), M(k_i + r)\right) \quad (32)$$

where: $\frac{\partial A_i}{\partial M(k_i + \ell)} = \frac{1}{\sqrt{E_{x_i} E_W}} M(k_i + \ell)$ (33)

whereas for $\frac{\partial \delta_i}{\partial M(k_i + r)}$ see (31).

Tab. II $c_i$ for the same windows of table I

| **Window** | Rectangular | Hanning | 4-terms Nuttal |
|---|---|---|---|
| $\frac{\partial \delta_i}{\partial \alpha_i}$ | $\frac{1}{(1+\alpha_i)^2}$ | $\frac{3}{(1+\alpha_i)^2}$ | $\frac{7}{(1+\alpha_i)^2}$ |

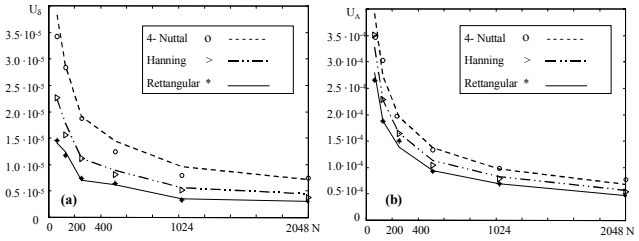


Fig. 1 δ uncertainty (a), and amplitude uncertainty (b) versus the number of point, N, for different windows, obtained with the IFFT algorithm (measured –symbols; estimated-line).

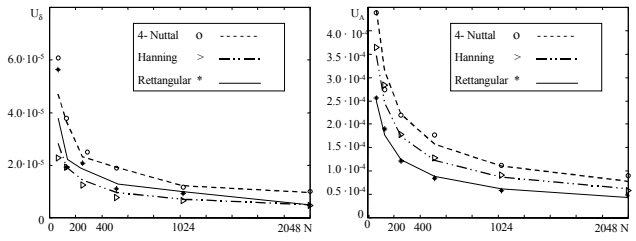


Fig. 2 δ uncertainty (a), and amplitude uncertainty (b) versus the number of point, N, for different windows, obtained with the energy-based approach (measured –symbols; estimated-line).

It is interesting to note from these relationships that whereas for the interpolated FFT the uncertainty formulas are linked to the window used via the sensitivity coefficient $\partial\delta_i/\partial\alpha_i$, for the other algorithm the relationships are independent form the window used.

## 4. NUMERICAL VALIDATION

This phase allows the results obtained in the theoretical analysis to be verified. It is carried out by running the proposed methods on data sets obtained by suitable model of the acquired system. In particular, the uncertainty was computed as the standard deviation of the output values obtained by considering a set of 100 input signals corrupted by the input uncertainty. Since it was proved that the main source of uncertainty in DFT algorithm is the quantization [11], the reported results concern input corrupted only by the quantization (see appendix A).

A meaningful evaluation of the obtained theoretical results requires the definition of some parameters concerning: hardware configuration (number of effective bit, B, full scale and time jitter of the A/D converter), operative condition (sampling frequency, number of elaborated point, N, used window, band, B) as well as characteristics of the input signal.

Figs. 1, 2, and 3 report the analytical results and the numerical ones concerning a 1 V amplitude, A, sinusoidal signal (f = 55 Hz) acquired at 800 Hz with an 1V full-scale A/D converter and using for the energy based algorithm K=5.
It has to be noted that the evaluated $U_A$ represents the minimum absolute uncertainty in these operating conditions having chosen the A/D full-scale equal to the signal amplitude. As to the frequency, it was chosen to present $U_\delta$ instead of $U_f$ since δ is always constrained in [-½; ½].

Uncertainty evolutions of δ, $U_\delta$, in function of N, having fixed B = 12 are reported in Figs. 1(a) and 2(a).

Analysing these two figures the following considerations can be carried out:

- uncertainty decreases with N;
- the analytical evolutions (lines) are in good agreement with the measured ones (symbols);
- the uncertainty obtainable with the two algorithms are very similar even if the $U_\delta$ obtained by using the energy-based approach is a little greater than the one obtained by using the interpolated FFT;
- as to the window used is concerned, better results are obtained with the Hanning and rectangular windows for the energy-based algorithm and for the interpolated FFT respectively. This last result is due to the very small equivalent noise bandwidth of the rectangular window [9]. Obviously in the choice of the window to be used also other parameters (e.g. the scallop loss rate, the sidelobe attenuation) have to be considered.

Analogously Figs. 1(b) and 2(b) show the amplitude uncertainty, $U_A$, evolutions in function of the number of processed points, N. Almost all the previously stated consideration are confirmed with only little differences. With the rectangular window $U_A$ is always less than the other windows. The uncertainties obtained by means the two algorithms are still very similar.

Further results are reported in Figs. 3, where the δ (a) and amplitude (b) uncertainty versus B, having fixed N = 128 are shown for the interpolated FFT algorithm. As you can see, the uncertainties decrease with B, with a saturation for B grater than 12.

## 5. CONCLUSIONS

The proposed theoretical and simulated approach to the evaluation of uncertainty of signal parameter estimated in frequency domain by two different algorithms allows some interesting considerations to be carried out:

- the uncertainty obtainable with both the considered algorithms are similar once the window has been chosen;
- the uncertainty decreases by increasing the number of elaborated points;
- the uncertainty due to the quantization decreases significantly by increasing the number of effective bit of the A/D up to 14 bit.

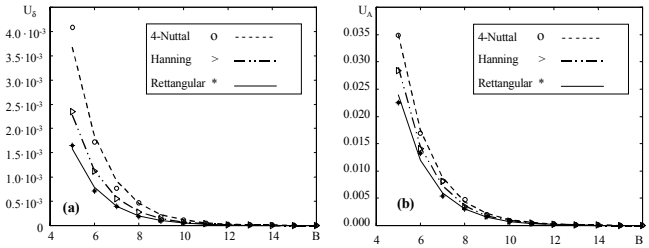


Fig. 3 δ uncertainty (a), and amplitude uncertainty (b) versus the A/D number of effective bit, B, for different windows, obtained with the interpolated FFT (Measured –symbols; estimated-line).

## APPENDIX A

The results obtained in [11] are summarised in the following. Said $U_{xm}$ the absolute uncertainty of each sample $x_m$, we have:

$$U^2_{R(k)} = \sum_{m=0}^{N-1}\left(\frac{\partial R(k)}{\partial x(m)}\right)^2 U^2_{x_m} = \frac{1}{S^2}\sum_{m=0}^{N-1} w^2(m)\cdot\cos^2(k\beta_m)U^2_{x_m}$$
$$U^2_{I(k)} = \sum_{m=0}^{N-1}\left(\frac{\partial I(k)}{\partial x(m)}\right)^2 U^2_{x_m} = \frac{1}{S^2}\sum_{m=0}^{N-1} w^2(m)\cdot\sin^2(k\beta_m)U^2_{x_m} \quad (A1)$$

and considering (3) and (4), general expressions for uncertainty on module and phase can be obtained:

$$U^2_{M(k)} = \frac{1}{S^2M^2(k)}\left[R^2(k)\sum_{m=0}^{N-1} w^2(m)\cos^2(k\beta_m)U^2_{x_m} + \right.$$
$$+ I^2(k)\sum_{m=0}^{N-1} w^2(m)\sin^2(k\beta_m)U^2_{x_m} + \quad (A2)$$
$$\left. - 2R(k)I(k)\sum_{m=0}^{N-1} w^2(m)\sin(k\beta_m)\cos(k\beta_m)U^2_{x_m}\right]$$

$$U^2_{\phi(k)} = \frac{1}{S^2M^4(k)}\left[R^2(k)\sum_{m=0}^{N-1} w^2(m)\cdot\sin^2(k\beta_m)U^2_{x_m} + I^2(k)\cdot\right. \quad (A3)$$
$$\left.\sum_{m=0}^{N-1} w^2(m)\cos^2(k\beta_m)U^2_{x_m} + 2R(k)I(k)\sum_{m=0}^{N-1}\sin(k\beta_m)\cos(k\beta_m)U^2_{x_m}\right]$$

These equations can be specified considering the uncertainties $U_{xm}$.

The uncertainty on each sample x(m) due to the quantization process performed by a real A/D converter can be posed equal to $U_{q:}$

$$U_q = V_{Range}\cdot 2^{-B}\Big/\sqrt{12} \quad (A4).$$

B is the effective bit number and $V_{Range}$ the A/D range[2].

The time jitter, can be modelled by adding to each ideal sampling instant $t_m$ a random variable uniformly distributed in the interval $[-J_\tau, +J_\tau]$; consequently [11] the uncertainty on each sample $x_m$ due to the time jitter is:

$$U_{J_m} = a_m\cdot J_\tau\Big/\sqrt{3} \quad (A5);$$

where $a_m$ is the first derivative of x(t) in the considered point.

The combined uncertainty on $x_m$ results:

$$U_{x_m} = \sqrt{U_q^2 + U_{J_m}^2} \quad (A7).$$

Considering only $U_q$ (A1)-(A2) become [11]:

$$U^2_{R(k)}\Big|_q = \frac{C_R(k)}{S}U_q^2;\ U^2_{I(k)}\Big|_q = \frac{C_I(k)}{S}U_q^2;$$
$$U^2_{M(k)}\Big|_q = \frac{\left(C_R(k)R^2(k) + C_I(k)I^2(k)\right)}{SM^2(k)}U_q^2 \quad (A8)$$

Where: $C_R(k) = \sum_{m=0}^{N-1} w^2(m)\cos^2(k\beta_m)/S$ ,. If $C_I(k)$ is equal $C_I(k) = \sum_{m=0}^{N-1} w^2(m)\sin^2(k\beta_m)/S$

to $C_R(k)$ we have: $U^2_{M(k)}\Big|_q = \frac{C_R(k)}{S}U_q^2$ (A9)

Tab. A1 - S, $C_R(k)$ and $C_I(k)$ values for the same windows of Tab. I.

| | | k=0; k=N/2 | k=1; k=N/2±1 k=N-1 | k=2; k=N/2±2 k=N-2 | k=3; k=N/2±3 k=N-3 | all other k |
|---|---|---|---|---|---|---|
| Rectangular S=N | $C_R(k)$ | 1.0000 | 0.5000 | 0.5000 | 0.5000 | 0.5000 |
| | $C_I(k)$ | 0 | 0.5000 | 0.5000 | 0.5000 | 0.5000 |
| Hanning S=N/2 | $C_R(k)$ | 0.7500 | 0.4375 | 0.3750 | 0.3750 | 0.3750 |
| | $C_I(k)$ | 0 | 0.3125 | 0.3750 | 0.3750 | 0.3750 |
| 4-Nuttal S=N*10/32 | $C_R(k)$ | 0.7219 | 0.5543 | 0.3867 | 0.3613 | 0.3609 |
| | $C_I(k)$ | 0 | 0.1676 | 0.3352 | 0.3605 | 0.3609 |

In Tab. A1 the values of S, $C_R(k)$ and $C_I(k)$ for the windows of Tab. I are reported.

## APPENDIX B

The covariance U((M(p),M(q)) between two module samples M(p) and M(q) can be obtained considering the dependence of both from the signal samples as follows:

$$U(M(p),M(q)) = \sum_{m=0}^{N-1}\frac{\partial M(p)}{\partial x_m}\frac{\partial M(q)}{\partial x_m}U^2_{x_n} =$$
$$= \sum_{m=0}^{N-1}\frac{U^2_{x_m}}{M(p)M(q)}\cdot\left[R(p)\cdot\cos(p\,\beta_m) + I(p)\cos(p\,\beta_m)\right]\cdot \quad (B1)$$
$$\cdot\left[R(q)\cos(q\,\beta_m) + I(q)\cos(q\,\beta_m)\right]$$


## ACKNOWLEDGMENTS

The author wishes to thank proff. Giovanni Betta and Antonio Pietrosanto for the useful suggestions and Ing. Maria Pacelli for the help given during the theoretical analysis.


## REFERENCES


[1] BIPM, IEC, IFCC, ISO, IUPAC, IUPAP, OIML, "Guide to the expression of uncertainty in measurement", 1993.

[2] G. Betta, C. Liguori, and A. Pietrosanto, "A structured approach to estimate the measurement uncertainty in digital signal elaboration algorithms", *IEE Proceedings-Part A* vol. 146, n.1, 1999, pp. 21-26.

[3] R.I. Becker and N. Morrison, "The errors in FFT estimation of the Fourier Transform", *IEEE Transactions on Signal Processing*, vol. 44, n. 8, 1996, pp. 2073-2077.

[4] J. Harris, "On the use of windows for harmonic analysis with the discrete Fourier transform", *IEE Proceedings*, vol. 66, n. 1, 1978.

[5] A. H. Nuttal, "Some windows with very good sidelobe behavior", *IEEE Trans. on ASSP*, vol. 29, n. 1, 1991, pp.84-91.

[6] L. Salvatore and A. Trotta, "Flat-top windows for PWM waveform processing via DFT", *IEE Proceedings*, vol. 135, n. 1, 1988, pp. 346-361.

[7] G. Andria, M. Savino, and A. Trotta: "Windows and interpolation algorithms to improve electrical measurement accuracy", *IEEE Trans. on Instrum. and Meas.*, vol. 88, n. 4, 1989, pp. 856-863.

[8] C. Offelli and D. Petri, "Interpolation techiniques for real-time multifrequency waveform analysis", *IEEE Trans. on I&M.*, vol. 39, n. 1, 1990, pp. 106-111.

[9] C. Offelli and D. Petri, "The influence of windowing on the accuracy of multifrequency signal parameter estimation", *IEEE Trans. on Instrum. and Meas.*, vol. 41, n. 2, 1992, pp. 256-261.

[10] C. Offelli and D. Petri, "A frequency domain procedure for accurate real-time signal parameter measurement," *IEEE Trans. on I&M.*, vol. 39, n. 1, 1990, pp. 106-111.

[11] G. Betta, C. Liguori, and A. Pietrosanto: "Propagation of Uncertainty in a Discrete Fourier Transform Algorithm", *Measurement*, vol. 27, May 2000, pp 231-239.